Evidence for Proton-Dominated Cosmic Ray Composition above 1.6 EeV

R.U. Abbasi,[1] T. Abu-Zayyad,[1] M. Al-Seady,[1] M. Allen,[1] J.F. Amman,[2] R.J. Anderson,[1] G. Archbold,[1] K. Belov,[1] J.W. Belz,[1,*] D.R. Bergman,[1,3] S.A. Blake,[1] O.A. Brusova,[1] G.W. Burt,[1] C. Cannon,[1] Z. Cao,[1] W. Deng,[1] Y. Fedorova,[1] C.B. Finley,[4] R.C. Gray,[1] W.F. Hanlon,[1] C.M. Hoffman,[2] M.H. Holzscheiter,[2] G. Hughes,[3] P. Hüntemeyer,[1] B.F Jones,[1] C.C.H. Jui,[1] K. Kim,[1] M.A. Kirn,[5] E.C. Loh,[1] J.P. Lundquist,[1] M.M. Maestas,[1] N. Manago,[6] L.J. Marek,[2] K. Martens,[1] J.A.J. Matthews,[7] J.N. Matthews,[1] S.A. Moore,[1] A. O'Neill,[4] C.A. Painter,[2] L. Perera,[3] K. Reil,[1] R. Riehle,[1] M. Roberts,[7] D. Rodriguez,[1] N. Sasaki,[6] S.R. Schnetzer,[3] L.M. Scott,[3] G. Sinnis,[2] J.D. Smith,[1] P. Sokolsky,[1] C. Song,[4] R.W. Springer,[1] B.T. Stokes,[1] S. Stratton,[3] S.B. Thomas,[1] J.R. Thomas,[1] G.B. Thomson,[1,3] D. Tupa,[2] L.R. Wiencke,[1] X. Zhang,[4] and A. Zech[3]

(The High Resolution Fly's Eye Collaboration)

[1] *University of Utah, Department of Physics, Salt Lake City, UT, USA*

[2] *Los Alamos National Laboratory, Los Alamos, NM, USA*

[3] *Rutgers University — The State University of New Jersey, Department of Physics and Astronomy, Piscataway, NJ, USA*

[4] *Columbia University, Department of Physics and Nevis Laboratory, New York, New York, USA*

[5] *Montana State University, Department of Physics, Bozeman, MT , USA*

[6] *University of Tokyo, Institute for Cosmic Ray Research, Kashiwa, Japan*

[7] *University of New Mexico, Department of Physics and Astronomy, Albuquerque, NM, USA*

Abstract

We report studies of ultra-high energy cosmic ray composition via analysis of depth of air-shower maximum (X_{max}), for airshower events collected by the High Resolution Fly's Eye (HiRes) observatory. The HiRes data are consistent with a predominantly protonic composition of cosmic rays at energies above 1.6 EeV ($10^{18.2}$ eV), when interpreted via the QGSJET01 and QGSJET-II high-energy hadronic interaction models. We measure a mean X_{max} at 10 EeV of 770.2 $\pm$ 2.1(stat.) $\pm$ 4.2(syst.) g/cm^2, and an elongation rate $dX_{max}/d(log(E))$ of 47.5 $\pm$ 5.9(stat.) $\pm$ 2.8(syst.) g/cm^2/decade. These measurements constrain models in which the galactic-to-extragalactic transition is the cause of the energy spectrum "ankle" at 4×10^{18} eV.

PACS numbers: 98.70.Sa, 95.85.Ry, 96.50.sb, 96.50.sd

*Corresponding author: belz@physics.utah.edu

The observation of a break in the cosmic ray energy spectrum at approximately 6×10^{19} eV [1, 2] provides strong evidence that the highest energy cosmic rays are both extragalactic and protonic [3, 4]. Direct evidence for a proton-dominated composition from airshower data would lend further support to this model, as would the observation of a transition from (heavy) galactic to (light) extragalactic cosmic rays at lower energies. A second feature, the "ankle" of the energy spectrum at 4×10^{18} eV may be indicative of this galactic to extragalactic transition or it may further strengthen the model in which the end of the cosmic ray spectrum is shaped by interactions with the cosmic microwave background [5]. Composition studies can provide decisive evidence in the choice between interpretations.

An important clue to chemical composition which is accessible to air fluorescence observatories is the depth of shower maximum X_{max} of cosmic ray induced extensive airshowers. Simple arguments [6, 7] show that the average value of airshower maximum $<X_{max}>$ will depend logarithmically on the primary energy and atomic mass, and that the *elongation rate* $d <X_{max}> / d \log E$ will be constant for unchanging primary compositions. Further, to first order, a nucleus-induced shower may be thought of as a superposition of showers induced by single nucleons. Therefore due to averaging effects we also expect the width of the X_{max} distribution at a given energy to be sensitive to the atomic mass of the primary.

The two fluorescence observatories of the High-Resolution Fly's Eye collected data in stereoscopic mode between December 1999 and April 2006. Located on the U.S. Army Dugway Proving Ground in Utah, at a mean elevation of 1,575 m MSL, a mean latitude of 40.16° N, and separated by 12.6 km, the observatories operated on clear moonless nights. Each detector consisted of an array of telescope modules, each module included a mirror of 3.7 m^2 effective area which focused UV light from airshowers on a 16×16 photomultiplier tube (PMT) camera. The field of view of each PMT subtended a one degree diameter cone of the sky. The HiRes-I detector covered nearly 360° in azimuth, 3°–17° in elevation and was read out by means of sample-and-hold electronics, while the HiRes-II detector covered 3°–31° in elevation and was read out by a custom FADC system [8].

The calibration of the HiRes telescope modules has been described previously [9]. A portable Xenon flash lamp ($\sim 0.5\%$ stability) was used to illuminate each mirror monthly. Between Xenon runs, night-to-night calibrations were performed using YAG laser light delivered to the PMT clusters via optical fiber. A pulsed nitrogen laser was fired into the atmosphere from various locations within 3.5 km of the two detector sites. An overall accu-

racy of $\sim 10\%$ RMS is achieved in the HiRes photometric scale.

Steerable lasers fired patterns of shots which covered the aperture of the HiRes fluorescence detectors, in order to monitor UV attenuation in the atmosphere. The vertical aerosol optical depth (VAOD) was measured to be 0.04(mean) $\pm$ 0.02(RMS), corresponding to a mean correction of $\sim$15% upward in energy for an event 25 km distant from the observatory. In the present analysis, the steerable laser measurements were used to compile an hourly atmospheric database and hence allow hourly tuning of the atmospheric parameters.

A mirror trigger was initiated if a sufficient number of PMTs were in temporal and spatial coincidence, then a stereo data set was obtained by the time-matching of HiRes-I and HiRes-II triggers. Geometrical reconstruction of stereo events proceeded by determination of the shower-detector plane from each HiRes site, the intersection of these two planes was taken to be the shower core trajectory. The resolution in the shower zenith angle is 0.6°, and the resolution in $R_{\rm p}$ (distance of closest approach to the detector) is 1.2%.

Hit information from multiple tubes in the HiRes-II data only are sorted into discrete time bins. In each bin, FADC signals are converted to a number of photoelectrons $N_{\rm pe}$, then adjusted for the effective area of each bin as determined by ray tracing. The geometry of the shower and the atmospheric databases are used to determine the atmospheric slant depth X for each shower bin. Shower segments that have emission angles within 5° of a bin's pointing direction are flagged and not used for fitting due to excessive Cherenkov light contamination. The $N_{\rm pe}$ profile is then converted to a profile of the fluorescence light at the shower by a routine that simulates the light production and propagation through the atmosphere, and subtracts the Cherenkov contribution.

The intensity of fluorescence light emitted from an airshower is proportional to the total ionization energy deposited by the charged particles in the shower [10]. We use the average fluorescence yield of several groups [11, 12, 13] and the spectral distribution given by Ref. [14], along with the average dE/dX determined from CORSIKA simulations [15] to determine the number of charged particles in the shower as a function of slant depth.

The shower profile is then fit to a Gaussian function of the age parameter $s(X) = 3X/(X + 2X_{\rm max})$ in order to determine the airshower energy and X_{max}. (Alternatively fitting by the Gaisser-Hillas parametrization [16] had little overall effect on the analyses and conclusions presented here.) Further details of the reconstruction used in this analysis are contained in Ref. [17].

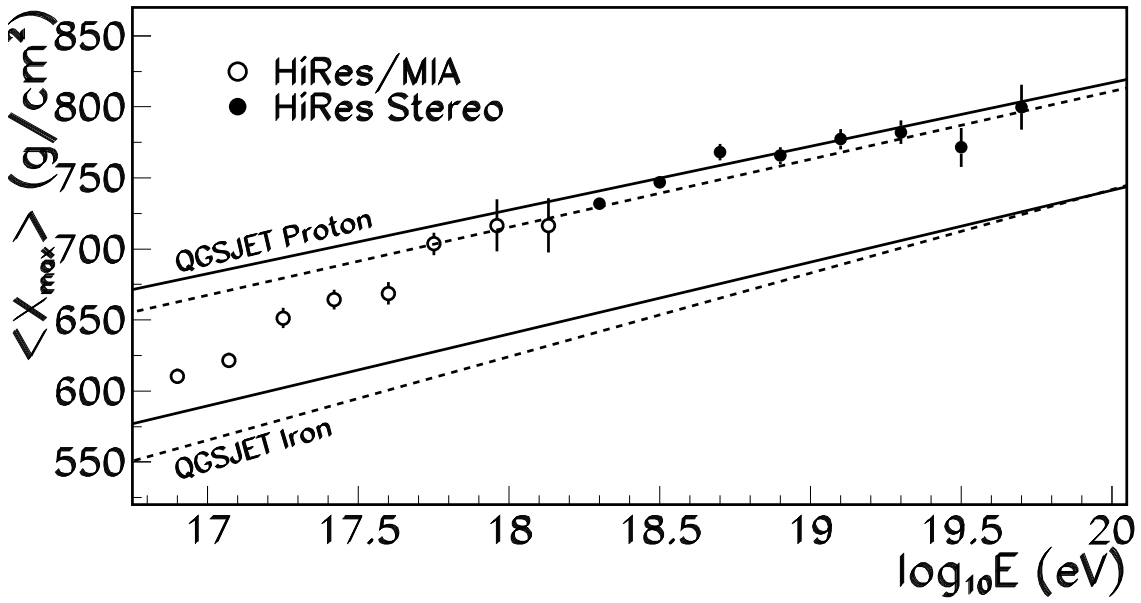

FIG. 1: Comparison of current HiRes stereo $< X_{max} >$ results with results from the HiRes-prototype/MIA hybrid [21]. Also included are QGSJET01 (dashed) and QGSJET-II (solid) predictions for pure-proton and pure iron compositions.

Ultra-high energy cosmic ray composition studies require a detailed comparison of data with the predictions of airshower models and are hence model dependent. In practice, these models are airshower Monte Carlo simulations. In order to completely understand the effects of the geometrical aperture of the detector, HiRes therefore applies a full detector simulation to the airshower Monte Carlo events.

HiRes uses a library of 32,000 (20,000) simulated proton- and iron-induced airshowers generated by the CORSIKA 6.003 (6.501) [15] package, using the QGSJET01 [18] (QGSJET-II [19]) hadronic interaction models and the EGS4 [20] electromagnetic interaction driver. Each shower is sampled at 205 points along its development, recording the number of particles at each slant depth. Airshower longitudinal development is fit to a Gaussian-in-Age (GIA) functional form, and its as-thrown X_{max} is recorded. The mean X_{max} as a function of energy, for airshowers in the HiRes shower library is shown in Figure 1.

Detector simulation proceeds by drawing an event from the shower library, assigning it a random core location and zenith and azimuthal angles and determining if it can trigger the detector. The number of charged particles at many discrete points along the shower

is then determined, and fluorescence light is then propagated from the shower to the detector. Light attenuation by the atmosphere is realistically simulated by using an hourly database describing the measured aerosol content, temperature, and pressure. Ray tracing is performed to determine which phototubes actually see the light, allowing for photocathode response and inactive space between PMTs. An electronics simulation then determines the pulse height and time for each tube for HiRes-I electronics and forms a FADC waveform for HiRes-II electronics. For all tubes the channel gains, DAC settings, thresholds and channel variances are simulated by using hourly database information. The same trigger algorithms used in hardware are simulated to determine if either detector triggers in monocular mode. If an event is triggered, the simulated data is written to disk in the identical format as real data, thereby allowing the study of Monte Carlo events by the same analysis chain. The HiRes Monte Carlo data set contains approximately 20 times the number of reconstructed stereo events as the data.

The major challenge in studying cosmic ray composition by the $<X_{max}>$ technique lies in understanding the systematic biases that occur during reconstruction and event selection. Low-energy showers which are nearby the detector may reach X_{max} above the field of view of the mirrors, thus biasing a data set towards deeper showers. High-energy showers with small zenith angles are likely to reach maximum below the field of view of the mirrors, resulting in a bias towards shallow showers.

It is useful to divide the types of biases which can occur into two types, called "acceptance biases" and "reconstruction biases". Acceptance biases are due to events which fail reconstruction altogether, including detector triggering and event selection effects. Reconstruction biases are due to events which are successfully reconstructed, but with the wrong X_{max}. The strategy in the following analysis is to choose event selection cuts which minimize the reconstruction bias, and make the acceptance bias as independent of energy as possible.

After geometrical reconstruction and fitting of the shower profiles to obtain energy and X_{max}, a set of cuts are applied in order to select an appropriate event sample. The chance probability that the event is due to noise must be less than 1%, and the χ^2/DOF of the fit must be less than 10. Data must have been taken in good weather conditions. Fit uncertainty in the zenith angle must be less than 2°, the fit uncertainty in X_{max} must be less than 100 g/cm^2, and the angular RMS with respect to the event plane of hit PMTs must be greater than 0.15°. The zenith angle of the event itself must be less than 70°, and

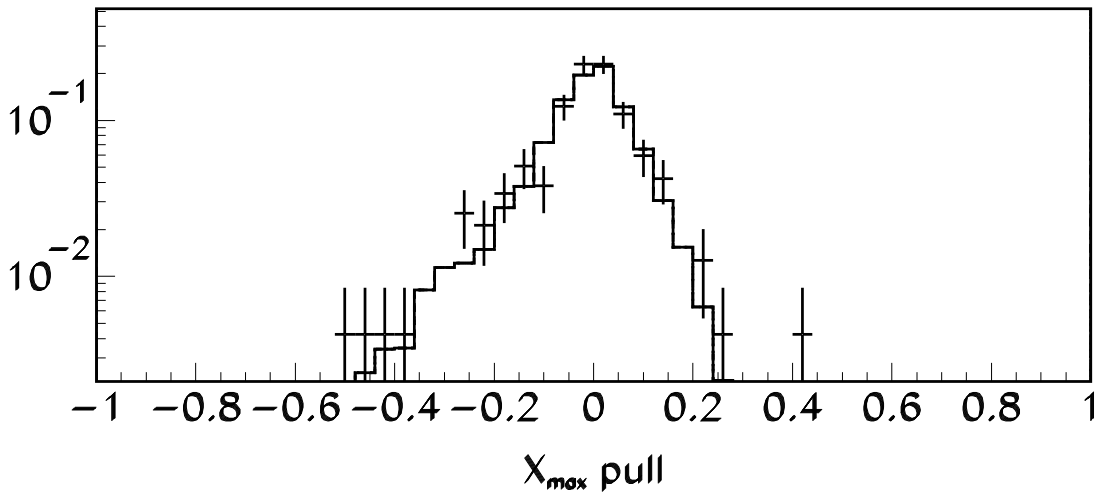

FIG. 2: X_{max} pull $= 2\times(X_{II}-X_I)/(X_{II}+X_I)$ (X_{II} and X_I are X_{max} as measured by HiRes-II and HiRes-I detectors, respectively) for HiRes stereo data (points) overlaid with QGSJET-II proton Monte Carlo. X_{max} bracketing by HiRes-I is required.

the $R_{\rm p}$ with respect to HiRes-II must be at least 10 km. Events are required to have X_{max} bracketed by the HiRes-II field of view, and have a shower-detector plane angle between 40° and 130°. Finally, events with energies $18.2 < \log(E(\text{eV})) < 19.8$ are selected for this analysis. A total of 1,126 events pass all cuts.

In Figure 2 the resolution in X_{max} of data and Monte Carlo events are compared by plotting the X_{max} "pull", defined as the difference between X_{max} measured by HiRes-I and X_{max} measured by HiRes-II divided by their average. The agreement between HiRes stereo and Monte Carlo pull distribution is excellent, including the asymmetry caused by HiRes-I covering only half the range in elevation angle. This justifies the use of Monte Carlo to determine X_{max} resolution, which is found to be better than 25 g/cm^2 over most of the HiRes energy range.

After application of the cuts above, an acceptance bias shifts the mean value of X_{max} for proton Monte Carlo events approximately 16 g/cm^2 below the shower library predictions. This bias is energy independent, independent of the choice of QGSJET01 or QGSJET-II high-energy hadronic model, and independent of the choice of GIA or Gaisser-Hillas fits to the shower profile. Based on the excellent agreement between the data and proton Monte Carlo predictions (*e.g.* Figure 3) a 16 g/cm^2 bias correction is applied to the data to obtain

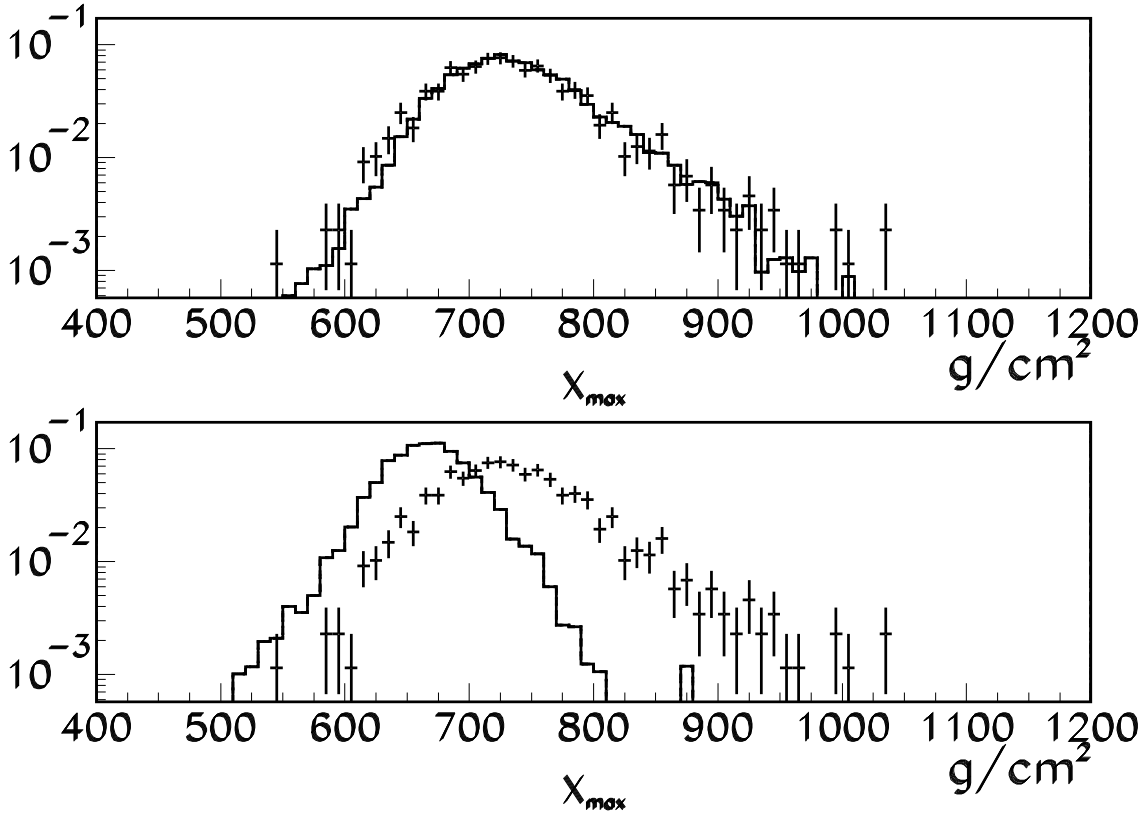

FIG. 3: *Top:* X_{max} overlay of HiRes data (points) with QGSJET-II proton Monte Carlo airshowers after full detector simulation. *Bottom:* X_{max} overlay of HiRes data (points) with QGSJET-II iron Monte Carlo airshowers after full detector simulation.

the $<X_{max}>$ points shown in Figure 1.

We assign a systematic uncertainty of 2.7 g/cm^2/decade to the elongation rate and 1.8 g/cm^2 on the absolute value of $<X_{max}>$ based on small variations of event selection cuts. Uncertainties in the energy do not have a large effect on elongation rate results due to the logarithmic energy scale. The choice of VAOD was the main systematic in a previous elongation rate analysis [22], however the use of an hourly atmospheric database in the present analysis renders this source of systematics negligible.

A systematic uncertainty of 0.7 g/cm^2 is assigned to the absolute value of $<X_{max}>$ due to the statistics of the Monte Carlo used in determining the acceptance correction. The Monte Carlo uncertainty in the energy dependence of this bias is approximately 1.8 g/cm^2/decade.

The phototube pointing directions have been confirmed by studies using stars [23] to within 0.3°, corresponding to a shift in X_{max} of approximately 15 g/cm^2. Averaging over

mirrors, this contributes a net uncertainty of 3.3 g/cm^2 to the value of $<X_{max}>$.

The subtraction of the Cherenkov light from the phototube signal can introduce an uncertainty in X_{max} due to uncertainties in electron multiple scattering. Previous studies [22] in which the width of the Cherenkov beam was varied by 2° (1 σ) indicated negligible effect on the elongation rate or absolute value of $<X_{max}>$.

In a linear fit with $\chi^2 = 9.1/(6$ df) we measure 47.5 ± 5.9(stat.)± 2.8(syst.) g/cm^2/decade for the elongation rate of ultra-high energy airshowers, and 770.2 $\pm$ 2.1(stat.) $\pm$ 4.2(syst.) g/cm^2 for the mean value of X_{max} at 10 EeV. These results are consistent with an unchanging proton dominated flux as compared to both the QGSJET01 and QGSJET-II models.

The fluctuations of X_{max} as a function of energy are also a probe of primary particle composition. Because the distributions tend to be both asymmetric and possess non-Gaussian tails however, care must be taken to use a suitable definition of the X_{max} width. The uncorrected RMS and sample standard deviations are biased estimators of the width [24] and tend to be subject to large fluctuations in distributions with broad tails.

In order to focus attention on the center of the X_{max} distribution and reduce sensitivity to fluctuations in the tails, the width is quantified as the width σ_X of a Gaussian where the distribution is truncated at $2 \times$ RMS in the unbinned likelihood fitting procedure. The results of this analysis applied to both the HiRes stereo data and to QGSJET-II proton and iron Monte Carlo are shown in Figure 4. The HiRes X_{max} width data are consistent with the predictions of QGSJET-II protons.

The distribution of QGSJET01 protons tends to be about 5 g/cm^2 broader than that of QGSJET-II protons, thus within QGSJET01 the HiRes X_{max} fluctuations appear slightly narrower than the pure proton prediction. However, studies of the full X_{max} distribution in which the data is modeled by a sum of QGSJET-like proton and iron distributions indicate that for both QGSJET01 and QGSJET-II the most likely proton fraction exceeds 90% over most of the HiRes energy range [25].

In conclusion, we report a 47.5 ± 5.9(stat.)± 2.8(syst.) g/cm^2/decade elongation rate and 770.2 ± 2.1(stat.) $\pm$ 4.2(syst.) g/cm^2 for the mean value of X_{max} at 10 EeV. The absolute value of $<X_{max}>$ as well as the observed fluctuations suggest a proton dominated cosmic ray flux above 1.6 EeV, within the QGSJET01 and QGSJET-II pictures. The HiRes X_{max} data places strong constraints on models in which the ankle is the result of a transition from

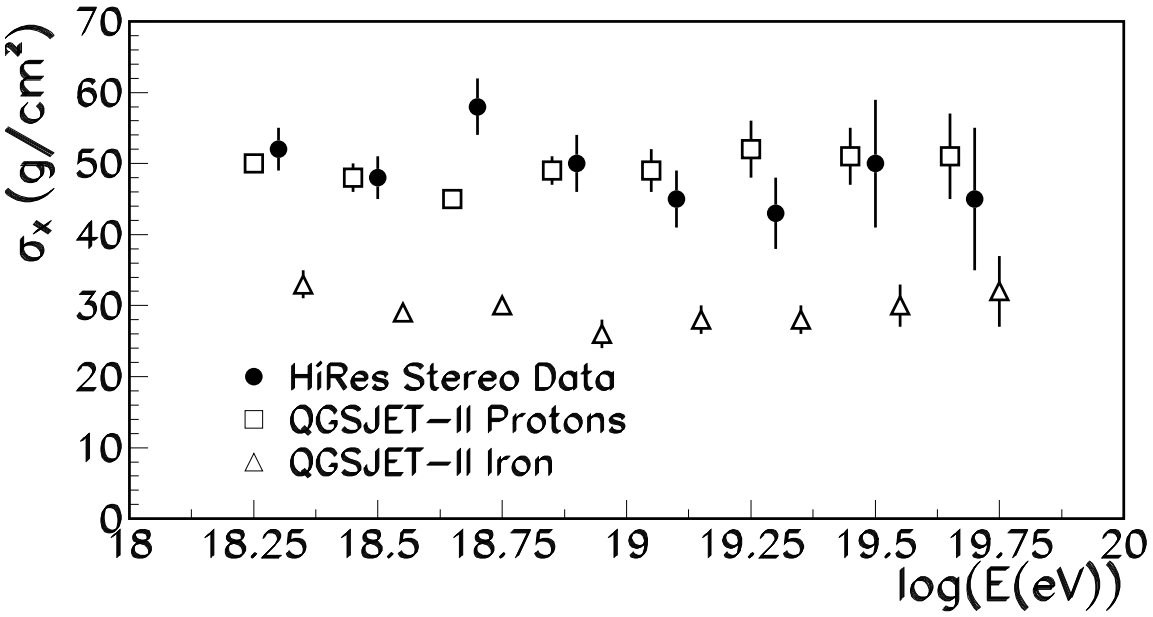

FIG. 4: Results of fitting HiRes stereo data X_{max} distribution to Gaussian truncated at $2 \times$ RMS (black points). Superimposed are expectations based on QGSJET-II proton (squares) and iron (triangles) Monte Carlo. Monte Carlo points are shown with small offsets in energy to provide separation.

heavy galactic to light extragalactic cosmic rays.

This work is supported by US NSF grants PHY-9321949, PHY-9322298, PHY-9904048, PHY-9974537, PHY-0098826, PHY-0140688, PHY-0245428, PHY-0305516, PHY-0307098, and by the DOE grant FG03-92ER40732.We gratefully acknowledge the contributions from the technical staffs of our home institutions. The cooperation of Colonels E. Fischer, G. Harter and G. Olsen, the US Army, and the Dugway Proving Ground staff is greatly appreciated.

---

[1] R. A. et al., Phys. Rev. Lett. **100**, 101101 (2008).

[2] J. A. et al., Phys. Rev. Lett. **101**, 061101 (2008).

[3] T. Greisen, Phys. Rev. Lett. **16**, 748 (1966).

[4] G. Zatsepin and V. Kuz'min, JETP Lett. **4**, 78 (1966).

[5] V. Berezinsky, in *Proc. 30th Intl. Cosmic Ray Conference* (Merida, Mexico, 2007).

[6] W. Heitler, *The Quantum Theory of Radiation* (Oxford University Press, 1954).

[7] J. Matthews, Astropart. Phys. **22**, 387 (2005).

[8] J. H. B. et al., Nucl. Inst. Meth. **A482**, 457 (2002).

[9] R. A. et al., Astropart. Phys. **23**, 157 (2005).

[10] J. B. et al., Astropart. Phys. **25**, 57 (2006).

[11] F. K. et al., Nucl. Inst. Meth. **A372**, 527 (1996).

[12] M. N. et al., Astropart. Phys. **20**, 293 (2003).

[13] J. B. et al., Astropart. Phys. **25**, 129 (2006).

[14] A. N. Bunner, Ph.D. thesis, Cornell University (1966).

[15] D. Heck and J. Knapp, Tech. Rep., Forschungszentrum Karlsruhe (2001).

[16] T. Gaisser and A. Hillas, in *Proc. 15th Intl. Cosmic Ray Conference* (Plovdiv, Bulgaria, 1997).

[17] W. F. Hanlon, Ph.D. thesis, University of Utah (2008).

[18] N. Kalmykov and S. Ostapchenko, Phys. Atom. Nucl. **56**, 346 (1993).

[19] S. Ostapchenko, Nucl. Phys. Proc. Suppl. **151B**, 143 (2006).

[20] W. N. et al., Tech. Rep. SLAC-265, Stanford Linear Accelerator Center (1985).

[21] T. A. et al., Ap. J. **557**, 686 (2001).

[22] R. A. et al., Ap. J. **622**, 910 (2005).

[23] P. S. et al., Astropart. Phys. **18**, 237 (2002).

[24] J. F. Kenney and E. S. Keeping, *Mathematics of Statistics, Pt. 2* (Van Nostrand, 1951), 2nd ed.

[25] J. Belz, in *Proc.* 21^{st} *Rencontres de Blois* (Blois, France, 2009).